Louise Steffensen Schmidt¹, Thomas V. Schuler¹, Sebastian Westermann¹, Tobias Dürig²

¹ Department of Geosciences, University of Oslo, Norway

²Institute of Earth Science, University of Iceland, Iceland

Correspondence: L. S. Schmidt < l.s.schmidt@qeo.uio.no>

ABSTRACT. The Arctic is undergoing increased warming compared to the global mean, with major implications for the mass balance of glaciers. Direct observations of mass balance in the Russian Arctic are sparse and remotely sensed volume changes do not provide information about climatic drivers. Here, we present simulations of the climatic mass balance and meltwater runoff from glaciers in Franz Josef Land and Novaya Zemlya from 1991-2022. Based on simulations of glacier climatic mass balance over the period 1991-2022, we present a first detailed view of mass balance evolution in Franz Josef Land and Novaya Zemlya. The simulations are conducted at a 2.5 km resolution using the CryoGrid model forced by the CARRA reanalysis product. Over the 30year simulation period, the climatic mass balance of both Franz Josef Land $(0.21 \text{ m w.e. a}^{-1})$ and Novaya Zemlya $(0.07 \text{ m w.e. a}^{-1})$ is positive on average without a significant trend in annual climatic mass balance. There is still a tendency towards more frequent high-melt years after 2010 and the associated glacier runoff has intensified with record melt years occurring during the model period.

INTRODUCTION

During the last decades, glaciers and ice caps worldwide have been melting at increasing rates as a response to a globally warming (e.g. Vaughan and others, 2013; Huss and Hock, 2018). The Arctic and particularly

This is an Open Access article, distributed under the terms of the Creative Commons Attribution licence (http://creativecommons.org/licenses/by/4.0), which permits unrestricted re-use, distribution and reproduction, provided the original article is properly cited.

the Barents Sea region, which includes the archipelagoes of Svalbard, Franz Josef Land, and Novaya Zemlya, has experienced pronounced warming (e.g. Screen and Simmonds, 2010; Lind and others, 2018; Carr and others, 2023). This warming is partly driven by a rapid sea ice decline, which leads to an enhanced heat transfer between the ocean and the atmosphere (e.g. Lind and others, 2018; Barton and others, 2018).

While there are several estimates of the climatic mass balance of Svalbard, both from in situ observations (e.g. Hagen and others, 2003; Schuler and others, 2020), satellite observations (e.g. Nuth and others, 2010; Moholdt and others, 2010; Mémin and others, 2011; Wouters and others, 2019) and modelling studies (e.g. Østby and others, 2017; Van Pelt and others, 2019; Schmidt and others, 2023), studies on the surface mass loss of Novaya Zemlya and Franz Josef Land are limited. In situ observation of mass balance and ablation were conducted sporadically from 1933-69 on the Shokal'ski Glacier in Novaya Zemlya (Zeeberg and Forman, 2001), but to our knowledge there are no recent in-situ estimates of the mass balance. There were reportedly also mass balance observation on Franz Josef Land until the early 1960's, although detailed measurements were hard to obtain (Dowdeswell and others, 1997).

There are, however, several estimates of the mass balance of both Novaya Zemlya and Franz Josef Land using geodetic methods, gravimetry, or both (e.g. Jacob and others, 2012; Moholdt and others, 2012; Ciracì and others, 2020; Tepes and others, 2021; Hugonnet and others, 2021; Sommer and others, 2022; Małecki, 2022). These estimates provide the total mass balance, including both the mass loss from glacier melting and frontal ablation. They mostly indicate a general mass loss from 2000-2019, with about -0.32 \pm 0.14 m w.e. a⁻¹ mass change in Novaya Zemlya and about -0.24 \pm 0.16 m w.e. a⁻¹ mass change in Franz Josef Land. The estimated average frontal ablation rate from 2000-20 has been estimated to be -0.15 \pm 0.05 m w.e. a⁻¹ for Novaya Zemlya and -0.71 \pm 0.33 m w.e. a⁻¹ for Franz Josef Land (Kochtitzky and others, 2022).

Modeling of the climatic mass balance, i.e. the sum of surface mass balance and internal mass change, can be an important tool to expand the time series beyond the observational period and to provide a detailed look at the mass balance components (the climatic mass balance, flux divergence, and frontal ablation) and climatic drivers. Information on glacial meltwater runoff can also be gathered from these models, which constitutes a significant source of the freshwater discharged into glacial fjords and coastal seas (Bamber and others, 2018). This freshwater discharge has important implication for a wide range of physical, chemical, and biological processes, including fjord circulation (Carroll and others, 2017), light availability (Hop and others, 2002; Arimitsu and others, 2012), water biogeochemisty (Wadham and others,

2013; Bhatia and others, 2013), and marine primary production (Juul-Pedersen and others, 2015; Hopwood and others, 2020).

The performance of these models needs to be assessed against observations, which are limited in the Russian Arctic. Some global models have provided estimates of the mass balance evolution using temperature as a proxy (e.g. Marzeion and others, 2012; Radić and Hock, 2011), but these are calibrated using only few observations in the Russian Arctic and may therefore have large uncertainties in this region. Only one previous study of all glaciers in the Arctic does provide estimates of the climatic mass balance and runoff using the regional climate model MAR (Maure and others, 2023), using ERA5 as model forcing and a horizontal model resolution of about 6 x 6 km.

Here, we present a high-resolution detailed estimate of the climatic mass balance and runoff from glaciers in Novaya Zemlya and Franz Josef Land at a high horizontal resolution (2.5 km x 2.5 km). We use the land surface model CryoGrid for the simulations, a full energy balance model coupled to a subsurface snow/firn scheme, with atmospheric forcings from the Copernicus Arctic Regional ReAnalysis (CARRA). The CryoGrid model is run for the same resolution as CARRA, eliminating the need for any additional downscaling. This model configuration has been well-validated for glaciers in Svalbard (Schmidt and others, 2023), and since glacier mass balance changes in the Russian Arctic has been found to closely mimic those of Svalbard (Lubinski and others, 1999), we expect reliable estimates for Novaya Zemlya and Franz Josef Land. The CARRA product currently spans from January 1991 to December 2022. For further validation, we evaluate the meteorological forcing against the few automatic weather stations available in the area, and compare our mass balance results to those found using geodetic methods (Hugonnet and others, 2021). Finally, the results of the climatic mass balance is compared to the other studies (e.g. Hugonnet and others, 2021; Kochtitzky and others, 2022; Maure and others, 2023).

STUDY AREA

The archipelagos of Franz Josef Land and Novaya Zemlya are situated in the north east and south east Barents Sea, respectively (Fig. 1a). The southern Barents Sea has a relatively mild and wet climate due to the strong influence of warm Atlantic waters, and the waters southwest of Novaya Zemlya are thus often ice-free, even in winter (Fig. 2a). The eastern coast of Novaya Zemlya borders to the Kara Sea, which, due to cold Arctic water and sea-ice coverage during winter and spring, experiences lower atmospheric temperatures than the southern Barents Sea region (Zeeberg and Forman, 2001). The Kara Sea coast also

has less precipitation than the Barents Sea coast.

Fig. 1. (a) The location of Franz Josef Land and Novaya Zemlya. (b+c) The position of land-terminating glaciers used for comparison with geodetic estimates (blue areas) and of the two automatic weather stations (yellow triangles) for (b) Franz Josef Land and (c) Novaya Zemlya.

The Atlantic influence is reduced in the northern Barents Sea, making Franz Josef Land the coldest and driest area in the region. The northern Barents Sea has previously been called the Arctic warming "hotspot" (Lind and others, 2018), due to the strongly amplified temperature increase in the region. This is linked to a decreasing trend in sea ice concentration in this area (Fig. 2c,d). Several processes and feedbacks contribute to the variations in sea ice around the Barents Sea. One important factor is the inflow of warm Atlantic water, which in combination with storm-induced ocean mixing has been shown to also affect sea ice variations (Duarte and others, 2020). Poleward atmospheric energy transport has also been shown to be an important factor (e.g. Olonscheck and others, 2019; Hofsteenge and others, 2022), with moisture transport in particular having a large impact on sea ice extent by increasing the downward longwave radiation and sensible heat flux (e.g. Doyle and others, 2011; Olonscheck and others, 2019; Fearon and others, 2021; Haacker and others, 2024). Atmospheric rivers and cyclones thus both contribute to sea ice variations, as both can cause extreme moisture and heat transport to the Arctic (e.g. Parker and others, 2022; Clancy and others, 2022; Li and others, 2024). Future sea ice loss can potentially increase and prolong

Fig. 2. (a-b) Average sea ice fraction in CARRA from 1991-2022 for (a) March and (b) September. Stippled areas have a zero sea ice concentration. The white line is the 15% threshold line. (c-d) Decadal trend in sea ice fraction from 1991-2022 in (c) March and (d) September. Stippled areas have no significant trend at a 95% confidence interval.

the intensity of cyclones, thus causing more extreme weather events (Parker and others, 2022).

Glacier cover is extensive for both Franz Josef Land (81%, or 13,000 km²) and Novaya Zemlya (27%, or 22,000 km²) (Fig. 1). The islands of Franz Josef Land are primarily covered with marine terminating ice caps, with only 4% of the ice area belonging to land-terminating glaciers. The elevations of the ice cap domes are generally 300-500 m a.s.l., but with a maximum ice elevation of 670 m a.s.l. (Barr and others, 1995). Novaya Zemlya consist of two main islands, the southern Yuzhny Island (maximum elevation of 1340 m) and the northern Severny Island (maximum elevation of 1596 m) (Kotlyakov and others, 2010). A large ice field, called the Northern Icefield, is situated on Severny island, which has outlet glaciers draining

into valleys and fjords. The Northern Icefield has an average elevation of 800 m (Grosvald and Kotlyakov, 1969), is more than 400 km long, with a mean width of 80 km (Rastner and others, 2017). In addition, small individual mountain glaciers are present on both main islands, and make up 7% of the total ice area (Małecki, 2022).

MATERIAL AND METHODS

CryoGrid community model

For simulations of the climatic mass balance and runoff, we use the CryoGrid community model (Schmidt and others, 2023; Westermann and others, 2023). CryoGrid is an open-source model developed for climate-driven simulations in the terrestrial cryosphere. It uses a full surface energy-balance model which can be coupled to different subsurface models of varying complexity. The model has a modular structure, with many different modules that can be combined to describe the evolution of subsurface temperature, water content and density for a wide range of surface and subsurface conditions. Information about the different functionalities and structures are described in detail by Westermann and others (2023). Three classes are used to describe the stratigraphy of glaciers in the Russian Arctic: a glacier (ice) module, a firn module and a snow module.

The glacier module consists of 47 layers of pure-ice with a user-defined constant ice thickness. Each layer has a thickness between 0.1 and 1 m, totaling of 20 m of ice. We assume a constant ice albedo of 0.4 for both Franz Josef Land and Novaya Zemlya. When mass is removed from the model by runoff, evaporation or sublimation, mass is shifted up from an infinite ice reservoir below into the lowest model layer. This is done to prevent the glacier from disappearing during long spin-ups due to the lack of ice flow. The infinite reservoir is assumed to have the same temperature as the lowest model layer.

If snowfall occurs during the simulation, a snow module is added on top of the glacier ice. In case the snow stays on the glacier surface for more than one year, the snow layer is relabeled as firn. The snow and firn schemes have the same model physics, and the distinction is mostly used to determine internal accumulation. The snow and firn modules follows a slightly altered Crocus (Vionnet and others, 2012) snow scheme as described by Westermann and others (2023) and Schmidt and others (2023). The mass balance model has a spectral albedo scheme which includes shortwave penetration, and also simulates the metamorphism and densification of snow and firn. Water percolation is controlled by a formulation for the hydraulic conductivity.

The full CryoGrid setup is described in detail by Schmidt and others (2023), and we refer to this paper for further details on the model.

Glacier outlines from the Randolph Glacier Inventory v 6.0 (Pfeffer and others, 2014) were used to compute a fractional glacier mask for both areas. We do not take into account changes in glacier extent during the study period.

Model forcing

2-D fields of meteorological forcing were extracted from the Copernicus Arctic Regional ReAnalysis (CARRA) dataset (Yang and others, 2021), including 2m air temperature, specific humidity, incoming long- and short-wave radiation, pressure, and precipitation. The CARRA dataset covers the European Arctic at a 2.5 x 2.5 km resolution, currently spanning from September 1990 to December 2022. It was created using the numerical weather prediction model HARMONIE-AROME (Bengtsson and others, 2017), which was forced at the lateral boundaries by ERA5 reanalysis. Here we use the east domain, which contains Svalbard, Franz Josef Land, Novaya Zemlya and Northern Norway. CARRA simulations have previously been validated and used as forcing for mass balance simulations of Svalbard glaciers (Schmidt and others, 2023). Sea ice in CARRA is represented by a one-dimensional thermodynamic sea ice scheme SICE (Batrak and others, 2018). The representation of the sea ice cover in CARRA has been found to significantly improve the sea ice surface temperature compared to ERA5, particularly in the winter in the Barents Sea region (Batrak and others, 2024).

The CARRA dataset is also used for calculating significant climatic trends for both areas. Throughout this paper, the term significance indicates p<0.05.

In-situ observations

Directly measured meteorological data are very sparse in both regions, and no Automatic Weather Station (AWS) observations are available from the glaciers of Franz Josef Land and Novaya Zemlya, but there are observations available from the archipelago. Air temperature, precipitation, relative humidity, and wind speed data were obtained from two AWS for forcing evaluation: E.T. Krenkelja (WMO ID: 20046) on Franz Josef Land and Malye Karmakuly (WMO ID: 20744) on Novaya Zemlya. These stations started observations in 1957 and 1876, respectively, and observations are currently available until mid-2021. The data were obtained from the Hydrometeorological Information World Data Centre Baseline Climatological

Data Sets (http://aisori-m.meteo.ru) and were provided at daily or 3-hour resolution. For the CARRA comparison we use daily values and only observations with a high-quality flag. For the E.T. Krekelja station on Franz Josef Land, around 18% of the time period has no valid data. The largest data gap is from August 2001 until November 2004. For Malye Karmakuly in Novaya Zemlya, only 1.8% of the period has no valid data. The location of the stations are shown in Fig. 1. It is important to note, that the temperature and relative humidity from these automatic weather stations are also assimilated into the CARRA product, and the correlation between CARRA and the observations may therefore be higher than for other regions on the archipelago.

Satellite observations

Geodetic mass balance

In the absence of in-situ measurements of mass balance, we instead use estimates of the geodetic mass balance for model validation. The geodetic mass balance is determined by taking the difference between glacier elevations at different survey dates to find the volume change rate. Using a value for the bulk density (often around 850 kg m⁻¹ (Huss, 2013)), this volume change is then converted into mass balance. Since the geodetic mass balance includes frontal ablation from marine-terminating glaciers, we only compare our climatic mass balance results to the geodetic balance of land-terminating glaciers, although the climatic mass balance of all glaciers in the regions are calculated with the model. All glaciers classified as land-terminating in the RGI are marked with blue in Fig. 1. The land-terminating glaciers are spatially distributed across the study areas, which is good for model validation.

Several studies have provided estimates of the geodetic mass balance of glaciers in Franz Josef Land and Novaya Zemlya (e.g. Moholdt and others, 2012; Tepes and others, 2021) but here we use the estimate by Hugonnet and others (2021). This study used Advanced Spaceborne Thermal Emission and Reflection Radiometer (ASTER) imagery for determining the geodetic mass balance of all glaciers on Earth from 2000-19. The results are available for all glaciers in the RGI at a temporal resolution of 1, 2, 4, 5, 10, and 20 years. In this study, we use the five year estimates for model evaluation.

Land surface temperature

In addition to the geodetic mass balance, we used observations of the land surface temperature (LST) from the Moderate Resolution Imaging Spectroradiometer (MODIS) on board the Terra and Aqua satellites to

provide an estimate of the melt frequency. The LST is provided at a 1 km resolution in the MOD11A1 (Terra) and MYD11A1 (Aqua) products with a daily resolution. For this study, observations from 2002-22 are used from the MODIS collection version 6. Tile h19v01 contains all glaciers on Novaya Zemlya, while Franz Josef Land is split between tile h18v01, h18v00, h19v01 and h19v00. We only use observations during the melt season, here assumed to be between 1 May and 1 October. To determine the amount of melt days, we calculate the maximum daytime LST from Terra and Aqua. MODIS LST has an uncertainty of at least $\pm 1^{\circ}$ C, and we therefore use -1°C as the threshold between melting and non-melting conditions (Hall and others, 2018). However, several studies have shown that MODIS has a larger cold bias in the Arctic (e.g. Hall and others, 2008a; Westermann and others, 2011; Østby and others, 2014), and this threshold may thus be too conservative. On average, between 28-47% of the investigated period has at least one daily cloud-free acquisition. To gap-fill any days that lack observations, we use a simple interpolation scheme. If a cloudy period is bookended by two melt days, we assume that the cloudy period also have melting conditions, as the LST usually is higher under cloud cover than under clear skies. A similar gap filling approach was used for Greenland by Hall and others (2008b). If the cloudy period is bookended by non-melt conditions, we assume that no melt occurred during the observation gap. If, on the other hand, the start of the cloudy period is preceded by a melt day and followed by a non-melt day, we assume half of the period has melt condition and the other half non-melt conditions. The uncertainties on the melt day estimate is calculated by assuming that for the latter case, the cloudy days are either all melt days or all non-melt days. This uncertainty estimate is likely conservative, as there is also uncertainties on the LST product itself, even during clear-sky days.

RESULTS

Evaluation

Figure 3 shows the comparison between the CARRA forcing and records of the two AWSs. The nearest point to the AWS on the CARRA grid is used for the comparison. The comparison with the 2m temperature (Figure 3(a,e)) shows that CARRA generally fits well with observations, with an average difference (model - observations) of -0.02° C for E.T. Krenkelja and -0.40° C for Malye Karmakuly. The root mean square error is approximately 1°C at both locations. The relative humidity (Figure 3(b)) is only measured at E.T. Krenkelja, with an average overestimation in CARRA of 0.76% and a root-mean-square-error of 8.3%. The windspeed is generally simulated well (Figure 3(c,f)), with a slight underestimation in CARRA of ~ -0.2 m



 s^{-1} and with root-mean-square-errors of ~ 5 m s^{-1} at both stations. The precipitation (Figure 3(d,g)) is overestimated at both locations, by 20% at the E.T. Krenkelja station and 86% at the Malye Karmakuly station. Precipitation gauges can severely undercatch precipitation, particularly during high wind events and for solid precipitation (Goodison and others, 1998; Yang and others, 2005), so some overestimation in the model results is to be expected. Still, the large difference for Malye Karmakuly could indicate an overestimation of the CARRA precipitation in Novaya Zemlya.

Fig. 4. The amount of melt days estimated by the CryoGrid model and from MODIS land surface temperatures. (a-b) The best estimates of the average amount of melt days per year from MODIS LST for (a) Franz Josef Land and (b) Novaya Zemlya. (c-d) The average differences in melt days from the MODIS estimate and the CryoGrid model. Positive values mean an overestimation in the CryoGrid model. (e-f) Timeseries of the amount of melt days. The grey areas shows the estimated uncertainty on the MODIS melt days and the black line shows the best estimate.

Figure 4 shows the average amount of melting days for all glacierized points, estimated using both CryoGrid and MODIS LST. The two estimates are generally close, with high correlation coefficients of 0.92 for Franz Josef Land and 0.88 for Novaya Zemlya. The CryoGrid estimate is generally within the uncertainty of the MODIS LST estimate. As previously mentioned, it is important to keep in mind that the uncertainties are most likely higher than reported here, due to the higher uncertainty of MODIS LST in the Arctic.

Figure 5(a-b) compares the simulated climatic mass balance and the geodetic mass balance by Hugonnet



and others (2021) for all glaciers from 2000 to 2020. Land terminating glaciers are marked with black. Since frontal ablation is not included in the simulations, all marine-terminating glaciers have a higher mass loss than in the simulations. Land-terminating glaciers are marked with black. Figure 5(c-d) shows the average climatic mass balance for all land-terminating glaciers. The simulated climatic mass balance is within the uncertainty estimate of the geodetic data for the whole period, although it is always above the best-estimate value. That the estimates for Novaya Zemlya are generally in the upper range of the uncertainty estimate could be consistent with the overestimation of modelled precipitation found for the Malye Karmakuly AWS.

Climatic trends

Since 1991, the CARRA simulations indicate positive trends in both temperature and precipitation over Franz Josef Land and Novaya Zemlya (Fig. 6). The average yearly temperature over Franz Josef land is -11.5°C, including both glacierized and non-glacierized land areas, with the highest average annual temperatures over low-elevation non-glacierized land (up to -4.4°C), and the lowest temperatures in the center of ice caps (down to -16.8°C). For Novaya Zemlya, the average yearly temperature is -8.2°C, with the highest average annual temperatures over non-glacierized land in the south (up to 0.5°C), and the lowest temperatures above high-elevation glacier points in the north (down to -16.4°C).

Particularly Franz Josef Land has experienced a significant warming (Fig. 6c), with a temperature trend of 1.8°C decade⁻¹. This is higher than the trend from both Novaya Zemlya (1.4°C decade⁻¹) and Svalbard (1.5°C decade⁻¹ (Schmidt and others, 2023) over the same period. The strongest temperature trends are found in the southern islands (up to 2.1°C decade⁻¹) while the lowest trends are found in the Northern islands (as low as 1.6°C decade⁻¹). For Novaya Zemlya (Fig. 6d), the largest temperature trends are found along the south and eastern coast (up to 2.1°C decade⁻¹), while the lowest trends are found along the western coast (down to 1.0°C decade⁻¹).

The average precipitation is 0.42 m w.e. a^{-1} over Franz Josef Land and 0.70 m w.e. a^{-1} over Novaya Zemlya. There is a significant trend in the average yearly precipitation for both locations of 0.05 m w.e. $decade^{-1}$. This is equivalent to a 15.1 % $decade^{-1}$ increase for Franz Josef Land and a 8.2 % $decade^{-1}$ for Novaya Zemlya, when compared to the 1991-2000 precipitation average. There is a significant positive trend in the precipitation for all points on Franz Josef Land (Fig. 6e), with a maximum trend at high elevation (up to 21 % $decade^{-1}$). For Novaya Zemlya (Fig. 6f), the highest trends are found in the northern



Fig. 7. (a-b) average yearly precipitation from 1991 to 2022 for all glaciers in the RGI for (a) Franz Josef Land and (b) Novaya Zemlya. (c-d) decadal trends in precipitation for all glaciers in the RGI for (a) Franz Josef Land and (b) Novaya Zemlya.

part of the archipelago (up to $20 \% \text{ decade}^{-1}$), with mostly insignificant trends in the South.

Figure 7 shows the average precipitation for each glacier in the RGI as well as the trend. For Franz Josef Land (Fig. 7a,c), glaciers on the southern islands generally receive the most precipitation. All glaciers have an increasing trend in precipitation. For Novaya Zemlya (Fig. 7b,d), the east-facing glaciers receive less precipitation than west-facing glaciers. The west-facing glaciers also have a larger increasing decadal trend than east-facing glacier, with the north-eastern glaciers experiencing the largest increase.

Climatic mass balance

Figure 8 shows the climatic mass balance of Franz Josef Land and Novaya Zemlya for the 1991/92 - 2021/22 glaciological years, defined as the period from September in the preceding to August in the current year.



Fig. 9. (a)-(b) Average climatic mass balance of all glaciers in the RGI from 1991/92 to 2021/22 for (a) Franz Josef land and (b) Novaya Zemlya. Note that both figures share the same colorscale. (c)-(d) boxplots of the climatic mass balance for glaciers in different area bins and histograms of the number of glaciers in each bin for (c) Franz Josef Land and (d) Novaya Zemlya.

We find that the climatic mass balance is generally positive over the simulation period, with an average climatic mass balance of 0.21 m w.e. a⁻¹ for Franz Josef Land and 0.07 m w.e. a⁻¹ for Novaya Zemlya. For some years, e.g. 2009/10 and 2013/14, the summer balance is even positive in both areas, due to low air temperatures and increased summer snow events. There is no significant trend in the annual climatic mass balance over the simulation periods, but there is a small, increasing trend in the winter mass balance for both areas. This amounts to an increase of 0.05 m w.e. decade⁻¹ for Franz Josef Land and 0.06 m w.e. decade⁻¹ for Novaya Zemlya. In general, there are more frequent high-melt years in the last decade, but only for Franz Josef Land is there a significant, but small, trend in the summer balance of -0.09 m w.e. decade⁻¹.

Figure 9 shows the average annual climatic mass balance for Franz Josef Land and Novaya Zemlya integrated for each glacier in the RGI. In addition, box plots of the average climatic mass balance is shown for different area bins. For Franz Josef Land (Fig 9a,c), the annual climatic mass balance of most glaciers is positive. Approximately 23% of all glaciers have a negative annual climatic mass balance, but since these are mostly small, they only account for 7% of the total glacier area. For Novaya Zemlya, 67% of the glaciers have a negative annual climatic mass balance. These are mostly glaciers with an area below 100 km², and thus only account for 35% of the total glacier area. West-facing glaciers have on average a higher climatic mass balance than East-facing glaciers. This is partly due to the higher precipitation in the East (Figure 7).

For both area, smaller glaciers have lower CMB than large glaciers, which is a similar behaviour as found for Svalbard (Schuler and others, 2020). The reason for this behaviour is partly that the smaller glacier have a lower accumulation area ratio (AAR) than the larger glaciers, as less of their area lies above the ELA. In addition, smaller glacier cover a smaller elevation span than larger glaciers, and often therefore do not reach as high accumulation.

Accumulation area ratio

The accumulation area of Franz Josef Land is large (Fig. 8a), with an average accumulation area ratio (AAR) of 78%. For a third of the period (10 years), the accumulation area encompasses almost the entire glacier area, with AAR > 95%. For most of the simulation period, the annual climatic mass balance is therefore positive, even with a positive summer balance during many years. One clear outlier is 2019/20, where an extremely negative summer mass balance is simulated. This leads to a very low AAR (9%) compared to the preceding years.

For Novaya Zemlya, the accumulation area ratio is on average 65%. Similar to Franz Josef Land, 2019/20 has a lower than average climatic mass balance and a low AAR (5%). Lower than average climatic mass balance and AAR has also been estimated for Svalbard (Schmidt and others, 2023), suggesting generally high melt rates in the Barents Sea region in 2019/20. However, some previous years (e.g. 2003/04 and 2012/13) have had comparable summer mass balance and AARs.

Refreezing and cold content

Figure 10 shows the changes in yearly refreezing, i.e. refreezing in the entire snow and firn column, and internal accumulation, i.e. refreezing below the annual layer. The average refreezing rate is similar for the two areas, of 0.23 m w.e. yr⁻¹ for Franz Josef Land and 0.24 w.e. yr⁻¹ for Novaya Zemlya. There is no significant change in the refreezing rate for Franz Josef Land, but there is a significant decrease for Novaya Zemlya of -0.018 m w.e. decade⁻¹. The internal accumulation accounts for on average 57% of the total refreezing for Franz Josef Land and 46% of the total refreezing for Novaya Zemlya. There is no significant trend for Franz Josef Land, but for Novaya Zemlya there is a significant decrease of -0.01 m w.e. decade⁻¹. The majority of the trend in the refreezing is therefore due to a decrease in internal accumulations, and there is no significant trend in the refreezing in the yearly layer.

The decrease in total refreezing is due to a decrease in the cold content of the snow and firn of Novaya Zemlya. Compared to the 1991-2000 average, the cold content at the beginning of the melt season (here defined as May 1st) has a significant decreasing trend of 10% decade⁻¹. As a result, the liquid water content at the beginning of the melt season has also significantly increased over the time period, with a trend of 0.42 m³m⁻³ decade⁻¹. Although there is no significant trend in the refreezing for Franz Josef Land, there is a significant trend in both the cold content and water content. The cold content has decreased by 6% decade⁻¹, while the liquid water content has increased by 0.43 m³m⁻³ decade⁻¹.

Fig. 10. The yearly specific refreezing (solid lines) and internal accumulation (stippled lines) for Franz Josef Land (blue) and Novaya Zemlya (red). The trend for Novaya Zemlya is shown in black. There is no significant trend for Franz Josef Land (p>0.05).

Runoff

There is a significant, increasing trend in the runoff from glaciers from both Franz Josef Land and Novaya Zemlya (Fig. 11). The runoff from Franz Josef Land over the simulation period is on average 0.24 m w.e. a^{-1} . There is a significant trend of 0.11 m w.e. $decade^{-1}$. The average for Novaya Zemlya is 0.76 m w.e. a^{-1} , with a significant trend of 0.20 m w.e. $decade^{-1}$. The runoff contribution from Novaya Zemlya is therefore much higher than that from Franz Josef Land, and the trend shows that the runoff has increased at almost twice the rate.

Fig. 11. The average specific runoff from 1991-2022 from glaciers in (a) Franz Josef Land and (b) Novaya Zemlya.(c) Time series of specific runoff (m w.e.) and trend.

The average runoff from each glacier in the RGI from 1991/92 to 2021/22 is shown in Figure 12, in addition to the runoff trend. For Franz Josef Land, all glaciers have an increasing runoff trend, with the

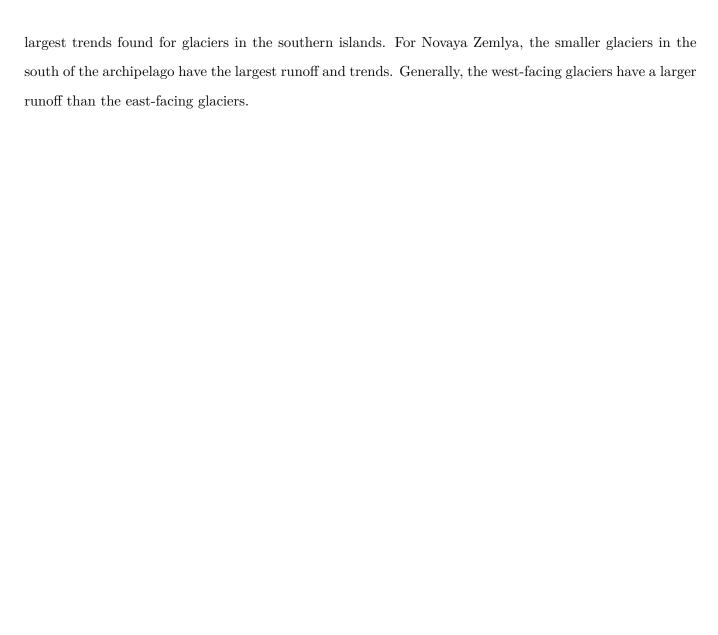


Fig. 12. Average runoff (a-b) and runoff trends (c-d) for each glacier in the RGI from 1991/92 to 2021/22 for (a,c) Franz Josef Land and (b,d) Novaya Zemlya.

Frontal ablation estimate

The mass balance simulations in this study only include surface and subsurface processes, but do not include glacier dynamics and frontal ablation. However, by comparing the climatic mass balance from this study with geodetic estimates, we can get an indication of the mass loss due to frontal ablation. Figure 8c,f shows the residuals between the geodetic estimate from Hugonnet and others (2021), including tidewater glaciers, and the climatic mass balance estimate simulated in this study. The residual comprises both

frontal ablation and the collective uncertainties in the geodetic and modelled mass balances. We assume that these residuals are only due to frontal ablation, and not due to errors in the climatic mass balance model. Thus, the residuals can provide a rough estimate of the frontal ablation. Based on these results, the frontal ablation rate of Franz Josef Land from 2000-19 is -0.49 ± 0.32 m w.e. a^{-1} . The residuals, and therefore the assumed frontal ablation rates, are fairly stable over the investigated period. For Novaya Zemlya, a similar frontal ablation rate is found from 2000-19 of -0.60 ± 0.47 m w.e. a^{-1} . The residuals vary throughout the investigated period, with the largest residuals in 2010-15. These estimates are consistent with the estimates by Kochtitzky and others (2022), which found frontal ablation rates of -0.71 ± 0.33 m w.e. a^{-1} for Franz Josef Land and -0.15 ± 0.05 m w.e. a^{-1} for Novaya Zemlya from 2000-20.

Model sensitivities

In order to explore the sensitivity of the model results to biases in the meteorological forcing, we apply uniform perturbations in temperature and precipitation for 1991 to 2022. Due to large computational cost, sensitivity simulations are only done for 50 points for each area, which were randomly selected across each of the domains. First, the air temperature is shifted by ± 0.5 and ± 1 °C, as the comparison between the modeled precipitation and two automatic weather stations had a root mean square error of 1 °C. Then precipitation is perturbed by ± 20 and $\pm 30\%$ (Table 1). For Franz Josef Land, comparison with an automatic weather stations showed a model bias of around 20%, while the model bias for the automatic weather station location in Novaya Zemlya was much higher, at 86%. However, this is likely partly due to undercatch, and we therefore limit this sensitivity test to 30%. A temperature increase of 1°C results in a decrease in the climatic mass balance of -0.37 for Franz Josef Land and -0.32 m w.e. a⁻¹ for Novaya Zemlya. This is similar to the sensitivity of -0.3 m w.e. a⁻¹ found for Svalbard (Van Pelt and others, 2012; Østby and others, 2017), but in the lower range of sensitivities for glaciers elsewhere in the world (Woul and Hock, 2005).

A 30% decrease in precipitation leads to a decrease in the climatic mass balance of -0.29 m w.e. a^{-1} for Franz Josef Land and -0.37 m w.e. a^{-1} for Novaya Zemlya. Novaya Zemlya is therefore slightly more sensitive to changes in precipitation. The effect of a 30% increase in precipitation is slightly less, with an increase in the climatic mass balance of 0.20 m w.e. a^{-1} for Franz Josef Land and 0.33 m w.e. a^{-1} for Novaya Zemlya.

Table 1. Sensitivity of the climatic mass balance (dB_{clim}) to perturbations in temperature and precipitation.

Parameter	Perturbation	Franz Josef Land		Novaya Zemlya	
		dB_{clim}	σ	dB_{clim}	σ
	$+ 1.0^{\circ} C$	-0.37	0.22	-0.32	0.19
Temperature	$+ 0.5^{\circ}\mathrm{C}$	-0.18	0.14	-0.15	0.10
	- 0.5°C	0.12	0.11	0.11	0.09
	- 1.0°C	0.20	0.16	0.21	0.15
	+ 30 %	0.20	0.16	0.33	0.13
Precipitation	+ 20 $%$	0.14	0.13	0.22	0.10
	- 20 %	-0.19	0.10	-0.24	0.11
	- 30 %	-0.29	0.16	-0.37	0.14

Extreme melt on Franz Josef Land in 2020

The large amount of melt from Franz Josef Land in 2020 in the simulations is largely due to high values of air temperatures, specific humidity, and incoming longwave radiation during the summer (June through August). The average energy balance during the summer is shown for each year in Figure 13.

In Franz Josef Land, the amount of melt is for most years controlled by the radiation balance, but in 2020 there was a large contribution from the turbulent fluxes. The average summer 2m temperature during 1991-2019 varied between -2 and -0.2°C, with an average value of -1°C. In 2020, on the other hand, the average 2m temperature reached 0.8°C. In combination with higher than average winds in some locations, the increase in the temperature gradient through the atmosphere leads to higher than usual sensible heat flux. The higher atmospheric temperatures are also followed by an increase in the incoming longwave radiation compared to previous years. The incoming shortwave radiation in June through August of 2020 is 12% below the average value, indicating cloudy conditions, but due to low glacier albedo the amount of absorbed shortwave is still above average.

The higher temperatures also lead to an increase in the specific humidity. From 1991-2019, the specific humidity during the summer varied between 0.0030 and 0.0036 g kg⁻¹ with an average of 0.0033 g kg⁻¹. In 2020, the average specific humidity was 0.0039 g kg⁻¹. The relative humidity was often 100%, meaning the hot, moist air had a higher specific humidity than the air close to the glacier surface. During some days, there is therefore a strong specific humidity gradient from a few meters above the surface towards the glacier ice surface, leading to deposition and a positive latent heat flux towards the surface.

The increase in both net longwave and shortwave radiation and turbulent fluxes leads to a larger amount of energy available for melt. On average during 1991-2019, the melt energy over the summer months was 23 W m^{-2} . The melt energy in summer 2020 was almost three times as high, at 66.6 W m^{-2} . Even in 2022, which is the year with the second highest melt energy over the summer months, the available energy is around two-thirds of that of 2020, at 44.6 W m^{-2} .

Fig. 13. The average contribution from individual energy balance components to the melt energy over glaciers from July through August in Franz Josef Land.

The temperatures from the AWS on Franz Josef Land in 2020 are consistent with the higher CARRA temperatures. From 1991-2019, the average yearly summer temperature at the AWS was between -1.1 and 0.7°C, with an average value for the whole period of around 0°C. In 2020, the average summer temperature was much higher at 1.2°C. In addition, an increase in melt days was found from the MODIS LST observations (Fig. 4c), corroborating the increase in melt in 2020.

Spatial variability in the Barents Sea region

The evolution of the climatic mass balance for the three land areas in the Barents Sea region - Svalbard, Franz Josef Land, and Novaya Zemlya - is shown in Fig. 14. For Svalbard, we show the range in climatic mass balance estimated from different modeling studies (Lang and others, 2015; Aas and others, 2016; Østby and others, 2017; Van Pelt and others, 2019; Noël and others, 2020; Schmidt and others, 2019), and calculate the average yearly climatic mass balance across the models. For Franz Josef Land and Novaya Zemlya, only the results from this study are shown. For the following discussion of climatic drivers, all climate variables (sea ice fraction, sea surface temperature etc) are taken from the CARRA reanalysis (Yang and others, 2021), as this is the forcing for the Cryogrid model.

The mass balance of the three archipelagos appear to be correlated for some of the period, particularly in the 1990s (Fig. 14a). All regions also experienced highly negative climatic mass balance in 2013 and 2020, which is linked to increased summer air temperatures and increased turbulent fluxes over glaciers in the areas, as well as a decreased sea ice fraction in the Barents Sea. For Novaya Zemlya, Haacker and others (2024) also found that the increased melt was due to increased turbulent fluxes, largely due to high fluxes of additional sensible heat, which was brought by atmospheric rivers and foehn winds. Atmospheric rivers can also lead to a decreased sea ice fraction in the Arctic (e.g. Li and others, 2024), and atmospheric rivers could therefore also be a contributing factor to the simulated decreased sea ice fraction in the Barents Sea during these years.

Although the annual mass balance is often similar for the three regions, there are large differences in both the summer and winter mass balance. Glaciers in Franz Josef Land generally have a less negative summer mass balance, but this is compensated by lower winter precipitation than in the other regions. Svalbard generally has the most negative summer climatic mass balance and highest winter climatic mass balance, while Novaya Zemlya lies in between. Still, even if the absolute values differ, there is a high correlation between the regions. In general, the annual climatic mass balance of Franz Josef Land is highly correlated to that of both Novaya Zemlya (r = 0.86) and Svalbard (r = 0.74), while the correlation between Novaya Zemlya and Svalbard is lower (r = 0.63). This high correlation is mostly controlled by the summer mass balance, where there is also a high correlation between all three regions (r > 0.6).

During some years there is a contrasting behaviour between the regions. For example, in 2001/02 and 2002/03 the amount of melt increased for Svalbard and the climatic mass balance thus became negative, while for both Franz Josef Land and Novaya Zemlya the climatic mass balance became positive. This is due

Fig. 14. (a) Specific climatic mass balance (cmb) and (b) cumulative climatic mass balance of glaciers in Svalbard, Franz Josef Land, and Novaya Zemlya. For Svalbard, the average and span in climatic mass balance from several modeling studies is shown (Lang and others, 2015; Aas and others, 2016; Østby and others, 2017; Van Pelt and others, 2019; Noël and others, 2020; Schmidt and others, 2019). Note that not all studies cover the entire study period. The lines from Franz Josef Land and Novaya Zemlya are the same as the green climatic mass balance lines in Fig. 8b,e.

to higher than average summer air temperatures over Svalbard and below-average summer air temperatures over Franz Josef Land and Novaya Zemlya, which lead to high turbulent fluxes and low albedo values over Svalbard. Conversely, in 2015/16 Novaya Zemlya experienced highly negative climatic mass balance which is not seen for Franz Josef Land and Svalbard. Both Franz Josef Land and Svalbard did experience increased melt in 2015/16, although not as extreme, and this increase in melt is partly out-weighted by an above average winter mass balance in these regions. This difference is also reflected in the average summer sea surface temperature (SST), as most of the CARRA domain experience higher-than-average SST but with the most extreme warming in SW Barents Sea and SE Kara Sea (see Fig. 15).

This contrasting behaviour does not appear to be directly linked to climate indicators, as we found that the correlation between modelled climatic mass balance (annual, summer and winter) and the North Atlantic Oscillation (NAO) and Artic Oscillation (AO) is low for all regions. We further investigated if the reason behind the contrasting behaviour could be found in the pressure patterns, sea ice extent,

wind patterns, or SST in the CARRA domain, but did not find a parameter which could explain all the variations, and it is therefore likely that the contrasting behaviour is due to a combination of different processes.

For 2002, 2003, 2009, and 2014, there are indications that the higher melt from Svalbard is due to increased Atlantic inflow. In these years, there is an above-average SST in the Norwegian Sea and the ocean areas around Svalbard during the summer months, while the eastern Barents sea experienced colder-than-average SST (see Fig. 15). This difference between Svalbard and the eastern Barents sea is particularly strong in 2002 and 2003, but this SST pattern is not evident in 2010 and 2017, where there is also contrasting behaviour between Svalbard and Franz Josef Land and/or Novaya Zemlya. The differences in 2010 and 2017 appear to be more related to longwave radiation and precipitation differences. In 2010 and 2017, while Novaya Zemlya experienced increased snowfall in summer, thus increasing the accumulation and the albedo, Svalbard received less-than-average summer snowfall. In addition, both Franz Josef Land and Novaya Zemlya received below-average incoming shortwave radiation over the summer. For 2010, the differences for Novaya Zemlya become more pronounced due to the addition of a high winter accumulation.

When calculating the cumulative climatic mass balance from 1991/92 to 2021/22 (Fig. 14b) there is a large span in the estimates for Svalbard, but on average Svalbard was losing mass over the simulation period while Franz Josef Land and Novaya Zemlya were gaining mass. A similar relation is found in the estimates of the total mass balance from Hugonnet and others (2021) for 2000-20, which found the largest relative mass loss from Svalbard (-0.31 \pm 0.09 m w.e. a^{-1}) followed by Novaya Zemlya (-0.25 \pm 0.10 m w.e. a^{-1}) and Franz Josef Land (-0.22 \pm 0.09 m w.e. a^{-1}).

DISCUSSION

Comparison to other studies

Only one other model estimate of climatic mass balance and runoff for the Russian Arctic based on energy balance modeling currently exists (Maure and others, 2023), which used the regional climate model Modèle Atmosphérique Régional (MAR) at a 6 km resolution. For the period 1991/92 to 2019/20, they found a climatic mass balance of -0.31 m w.e. a^{-1} for Novaya Zemlya and 0.16 m w.e. a^{-1} for Franz Josef Land. In this study, we find very similar values of climatic mass balance for Franz Josef Land for this period (0.22 m w.e. a^{-1}), but there are significant differences for Novaya Zemlya, where this study finds a much less negative yearly climatic mass balance (0.06 m w.e. a^{-1}). This difference could be due to differences in

temperature and precipitation type between the two products for Novaya Zemlya. Differences between the two models could both stem from the different resolutions (2.5 km for this study vs 6 km for MAR) and from differences in model physics and parameterizations. For example, MAR uses the hydrostatic approximation while CARRA uses a non-hydrostatic model. Previous studies have shown that a non-hydrostatic model may provide more accurate estimates of precipitation (e.g. Kato and Saito, 1995; Schmidt and others, 2018; Liu and others, 2022). Nevertheless, the average total precipitation for the two studies is similar over glaciers in Novaya Zemlya, but the amount of rainfall is much higher in the MAR product than for the CryoGrid simulations. In terms of the runoff, Maure and others (2023) finds values of 1.16 m w.e. a⁻¹ for Novaya Zemlya and 0.32 m w.e. a⁻¹ from Franz Josef Land. In this study, we find a lower average runoff for both regions, with 0.76 m w.e. a⁻¹ from Novaya Zemlya and 0.23 m w.e. a⁻¹ from Franz Josef Land.

Several studies have provided estimates of the geodetic mass balance (e.g. Jacob and others, 2012; Moholdt and others, 2012; Ciracì and others, 2018; Hugonnet and others, 2021). These studies all found that glaciers in Franz Josef Land and Novaya Zemlya have been loosing mass over the last decades, which seems to contradict the on average positive climatic mass balance found for these regions. Considering the large contribution of frontal ablation, these results are not necessarily in contradiction. For example, for 2000 to 2020, Franz Josef Land had a mass balance of -0.22 ± 0.09 m w.e. a^{-1} and Novaya Zemlya had a mass balance of -0.25 ± 0.10 m w.e. a^{-1} , according to Hugonnet and others (2021). For the same period (2000 to 2020), the frontal ablation was equal to -0.71 ± 0.33 m w.e. a^{-1} for Franz Josef Land and -0.15 ± 0.05 m w.e. a^{-1} for Novaya Zemlya (Kochtitzky and others, 2022). This means that the estimated climatic mass balance for Franz Josef Land is 0.49 ± 0.42 m w.e. a^{-1} , and thus, even when uncertainties are taken into account, the climatic mass balance of Franz Josef Land over this period is likely to be positive. For comparison, this study finds an average annual climatic mass balance of 0.21 m w.e. a^{-1} .

The estimate of the climatic mass balance of Novaya Zemlya, on the other hand, is -0.10 ± 0.15 m w.e. a^{-1} , and could therefore either be positive or negative. A positive mass balance for this period of 0.07 m w.e. a^{-1} for Novaya Zemlya, as found in this study, is therefore just outside the uncertainty estimate. As previously mentioned, comparisons with automatic weather stations indicate that the meteorological forcing has an overestimation in precipitation, which could lead to this overestimation in the climatic mass balance.

For Novaya Zemlya, the surface mass loss over the last decade has been found to be largely due to high

melt years in 2013, 2016, 2020, and 2022 (Haacker and others, 2024), which is consistent with this study. The most extreme melt events were due to a combination of atmospheric rivers and foehn winds (Haacker and others, 2024).

Uncertainties

Although we have tried to limit the uncertainties in the mass balance estimate by using a model which has previously been validated over Svalbard and a high-resolution reanalysis product as model forcing, several sources of uncertainty affect the results presented in this study.

First, there are uncertainties associated with the CARRA reanalysis. Although it showed a good fit with in-situ measurements of meteorological variables on glaciers on Svalbard (Schmidt and others, 2023), fewer observations are available for assimilation over the Russian Arctic, which can affect the accuracy. A comparison with two available weather stations was performed, but these are also assimilated into the CARRA product and may not represent the uncertainties of other areas. The comparison did show that precipitation is likely the largest source of uncertainty, with both AWSs indicating an overestimation of precipitation, particularly for Novaya Zemlya (86%). Considering that the climatic mass balance of Novaya Zemlya was only found to be slightly positive (0.07 m w.e. a⁻¹), if this comparison is indicative for the rest of the archipelago, it is likely that the climatic mass balance is actually negative. Still, regional extrapolation of precipitation from just one weather station is particularly tenuous. For the automatic weather station in Franz Josef Land, a much smaller precipitation overestimation of 20% was found, and part of the precipitation difference can likely be explained by undercatch. It is not surprising that precipitation is a big source of uncertainty, as precipitation generally is the hardest value for climate models to capture, and many previous modeling studies in the arctic has found large biases for this variable (e.g. Forbes and others, 2011; Schmidt and others, 2017; Van Pelt and others, 2019; Lenaerts and others, 2020).

Second, there are uncertainties associated with the model physics and setup. Although the CryoGrid glacier scheme has previously been validated over Svalbard (Schmidt and others, 2023), and we therefore expect the model to perform well in the similar climatic conditions of the Russian Arctic, there are always uncertainties in the models formulations. For example, the albedo and snow densification schemes are based on Crocus (Vionnet and others, 2012), which was developed for glaciers in the alps and not in the Arctic. Several studies have shown that Crocus struggle to properly simulate profiles of density in Arctic snowpacks (Royer and others, 2021; Barrere and others, 2017; Lackner and others, 2022), for example due

to an underestimation of wind-induced compaction. Although modifications were added to the model to better simulate Arctic conditions following Royer and others (2021), the model still struggles to simulate firn compaction (Innanen, 2023). Although the model performs well when compared to geodetic estimates, large errors occasionally occur for individual glaciers. In addition, we use a 30-year spin-up to initialize the sub-surface conditions before the start of our simulations. This was done by repeating the forcing from 1991-2000, which could introduce biases in both the extent and depth of the firn, as in reality the glaciers were most likely not in balance with the 1991-2000 climate.

Third, we neglect the effect of ice flow and glacier geometry changes on the mass balance by assuming fixed glacier outlines and a static elevation model. Both areas are based on observations collected between 2000-10 (Pfeffer and others, 2014; Schyberg and others, 2020) and should therefore be representative for most of the investigated period. A fixed elevation model may still introduce a negative bias in the beginning of our study period, as the elevation may be too low, and a positive bias towards the end of the study period where the used elevation model may be too high. The glacier elevation decreased by an average of $-0.26\pm0.10~\mathrm{m~a^{-1}}$ in Franz Josef Land and $-0.30\pm0.11~\mathrm{m~a^{-1}}$ in Novaya Zemlya from 2000-20 (Hugonnet and others, 2021). From 1952-2013, a similar thinning rate for Novaya Zemlya of -0.26 ± 0.04 m a⁻¹ was found (Melkonian and others, 2016). Based on these values, and considering the elevation map used in this study is based on observations from the 2000s, we expect maximum average deviation to be 8 m. From 1991 to 2023, we find average changes of mass balance with elevation of $2.6 \cdot 10^{-3}$ m w.e. m⁻¹ for Franz Josef Land and $2.0 \cdot 10^{-3}$ m w.e. m⁻¹ for Novaya Zemlya. We thus expect the error associated with the constant glacier mask to be less than 0.02 m w.e. a^{-1} on average. In areas where the thinning rate is higher than the average, the associated errors may be larger. For Novaya Zemlya, the thinning rate is largest near the glacier front, with high average frontal thinning of e.g. -0.92 m a⁻¹ from 2003-09 (Moholdt and others, 2012). The thinning pattern for Franz Josef Land is more erratic, with strong glacial thickening in some areas and strong glacial thinning confined to a small number of glaciers (Moholdt and others, 2012; Sommer and others, 2022).

Using a fixed glacier geometry means we do not account for frontal retreat or advance. Even small changes in glacier geometry can lead to significant variations in the total climatic mass balance, especially in the lower ablation zone, where melt rates are highest (e.g. Østby and others, 2017). Outlines of glaciers at various time intervals are available through the Global Land Ice Measurements from Space (GLIMS) database (GLIMS Consortium, 2005; Raup and others, 2007), though outlines are only available after 2000

for these areas. For Franz Josef Land, we create a glacier mask for the early 2000s (a mixture of outlines from 2002-06) and for 2016. Our analysis shows that using these two different glacier masks, which are about 10 years apart, results in an average change in climatic mass balance of only 0.4%. For Novaya Zemlya, we establish a glacier mask for the early 2000s (2002-04) and for 2019. The analysis indicates an average difference in climatic mass balance of 5.4% between these masks, which are approximately 15 years apart. While limited information is available on the frontal position of glaciers in Franz Josef Land, Novaya Zemlya has shown greater retreat from 2000-20 compared to earlier decades (Carr and others, 2023). Therefore, we assume that errors due to geometry changes are smaller before 2000 than the values we found here.

CONCLUSION

We present a detailed estimate of the climatic mass balance of Franz Josef Land and Novaya Zemlya, simulated with a full energy balance model at a 2.5 x 2.5 km horizontal resolution from 1991 to 2022. These results provide an estimate of the changes in runoff and climatic mass balance, in a region where temperatures are increasing at high rates but not many in-situ observations are available. These results may therefore be useful to estimate e.g. changes in the freshwater input from glacier runoff to the Barents Sea region.

In the model simulations, we find no significant trend in the annual climatic mass balance over the simulation period, 1991/92 to 2021/22, for both Novaya Zemlya and Franz Josef Land. The average climatic mass balance is positive for both regions, with values of 0.21 m w.e. a^{-1} for Franz Josef Land and 0.07 m w.e. a^{-1} for Novaya Zemlya, but there is a tendency towards more frequent high melt years after 2010. By comparing our results to the geodetic estimate by Hugonnet and others (2021), we get an estimate of the frontal ablation rate from 2000-19 of -0.49 ± 0.32 m w.e. a^{-1} for Franz Josef Land and -0.60 ± 0.47 m w.e. a^{-1} for Novaya Zemlya. Thus, due to the large contribution of frontal ablation in these regions, the glaciers in these areas are still losing mass on average.

We find that glaciers in both regions experienced extreme mass loss in 2013, 2020, and 2022, due to high summer air temperatures and an increase in the contribution of turbulent fluxes. These extreme melt years coincide with years of low sea ice extent in the Barents Sea region. On the other hand, in e.g. 2009/10 and 2013/14 the simulations show strong positive mass balance, even during the summer. In these years, glaciers in both areas experienced above-average winter accumulation, in addition to below average

summer melt due to low air temperatures and summer snow events.

Although there is no significant trend in the annual climatic mass balance, there is a significant increasing trend in the glacier runoff from both regions. The largest trend is found in Novaya Zemlya of 0.20 m w.e. a^{-1} . A smaller, but still significant, trend is found for Franz Josef Land, of 0.11 m w.e. decade⁻¹. The average runoff over the simulation period is 0.24 m w.e. a^{-1} for Franz Josef Land and 0.76 m w.e. a^{-1} for Novaya Zemlya.

In general, we find that 2020 was a year with highly negative mass balance, with particularly Franz Josef Land experiencing an extreme melt year. This is attributed to an increase in the sensible heat flux and a decrease in radiative cooling.

DATA AND CODE AVAILABILITY

The simulations described in this paper at monthly and daily resolutions are available at

https://doi.org/10.21343/k5gq-bh33 (Schmidt, 2023). They can be used for a wide range of applications, e.g. as input for runoff, ocean circulation or ecosystem models.

CARRA data (Schyberg and others, 2020) was downloaded from the Copernicus Climate Change Service (C3S) Climate Data Store. The results contain modified Copernicus Climate Change Service information 2022. Neither the European Commission nor ECMWF is responsible for any use that may be made of the Copernicus information or data it contains.

The CryoGrid community model is hosted on Github. The source code is available at https://github.com/CryoGrid/CryoGridCommunity_source.

ACKNOWLEDGMENTS

We are grateful to Lara Ferrighi and Øystein Godøy for their valuable help with data archiving. The research conducted in this study was funded by the Research Council of Norway through the Nansen Legacy project (NFR-276730). The simulations were performed on resources provided by the Department of Geosciences, University of Oslo. We thank the editor Shad O'Neel and two anonymous reviewers for their constructive comments, which improved the clarity of this manuscript.

REFERENCES

- Aas KS, Dunse T, Collier E, Schuler TV, Berntsen TK, Kohler J and Luks B (2016) The climatic mass balance of Svalbard glaciers: a 10-year simulation with a coupled atmosphereglacier mass balance model. *Cryosphere*, **10**(3), 1089–1104, ISSN 1994-0424 (doi: 10.5194/tc-10-1089-2016)
- Arimitsu ML, Piatt JF, Madison EN, Conaway JS and Hillgruber N (2012) Oceanographic gradients and seabird prey community dynamics in glacial fjords. Fish. Ocean., 21(2-3), 148–169, ISSN 10546006 (doi: 10.1111/j.1365-2419.2012.00616.x)
- Bamber JL, Westaway RM, Marzeion B and Wouters B (2018) The land ice contribution to sea level during the satellite era. *Environ. Res. Lett.*, **13**(6), 063008, ISSN 1748-9326 (doi: 10.1088/1748-9326/aac2f0)
- Barr S, Hisdal V, Lefauconnier B, Glazovskij AF, Safronova IN, Weslawski H Jan-Marcin Slupetzky, Krenke AN and Hansson R (1995) Franz Josef Land. ISBN 82-7666-095-9
- Barrere M, Domine F, Decharme B, Morin S, Vionnet V and Lafaysse M (2017) Evaluating the performance of coupled snow-soil models in SURFEXv8 to simulate the permafrost thermal regime at a high Arctic site. *Geosci. Model Dev.*, **10**(9), 3461–3479, ISSN 19919603 (doi: 10.5194/GMD-10-3461-2017)
- Barton BI, Lenn YD and Lique C (2018) Observed atlantification of the Barents Sea causes the Polar Front to limit the expansion of winter sea ice. J. Phys. Ocean., 48(8), 1849–1866, ISSN 15200485 (doi: 10.1175/JPO-D-18-0003.1)
- Batrak Y, Kourzeneva E and Homleid M (2018) Implementation of a simple thermodynamic sea ice scheme, SICE version 1.0-38h1, within the ALADINHIRLAM numerical weather prediction system version 38h1. *Geosci. Model Dev.*, 11(8), 3347–3368, ISSN 1991-9603 (doi: 10.5194/gmd-11-3347-2018)
- Batrak Y, Cheng B and Kallio-Myers V (2024) Sea ice cover in the Copernicus Arctic Regional Reanalysis. *Cryosphere*, **18**(3), 1157–1183, ISSN 1994-0424 (doi: 10.5194/tc-18-1157-2024)
- Bengtsson L, Andrae U, Aspelien T, Batrak Y, Calvo J, de Rooy W, Gleeson E, Hansen-Sass B, Homleid M, Hortal M, Ivarsson KI, Lenderink G, Niemelä S, Nielsen KP, Onvlee J, Rontu L, Samuelsson P, Muñoz DS, Subias A, Tijm S, Toll V, Yang X and Køltzow MØ (2017) The HARMONIEAROME Model Configuration in the ALADINHIRLAM NWP System. *Mon. Weather. Rev.*, **145**(5), 1919–1935 (doi: 10.1175/MWR-D-16-0417.1)
- Bhatia MP, Kujawinski EB, Das SB, Breier CF, Henderson PB and Charette MA (2013) Greenland meltwater as a significant and potentially bioavailable source of iron to the ocean. *Nat. Geosci.*, **6**(4), 274–278, ISSN 17520894 (doi: 10.1038/ngeo1746)
- Carr R, Murphy Z, Nienow P, Jakob L and Gourmelen N (2023) Rapid and synchronous response of outlet glaciers to ocean warming on the Barents Sea coast, Novaya Zemlya. *J. Glaciol.*, ISSN 00221430 (doi: 10.1017/jog.2023.104)

- Carroll D, Sutherland DA, Shroyer EL, Nash JD, Catania GA and Stearns LA (2017) Subglacial discharge-driven renewal of tidewater glacier fjords. J. Geophys. Res. Ocean., 122(8), 6611–6629, ISSN 21699275 (doi: 10.1002/2017JC012962)
- Ciracì E, Velicogna I and Sutterley TC (2018) Mass Balance of Novaya Zemlya Archipelago, Russian high arctic, using time-variable gravity from GRACE and altimetry data from ICESat and CryoSat-2. Remote. Sens., 10(11), 1817, ISSN 20724292 (doi: 10.3390/rs10111817)
- Ciracì E, Velicogna I and Swenson S (2020) Continuity of the Mass Loss of the World's Glaciers and Ice Caps From the GRACE and GRACE Follow-On Missions. *Geophys. Res. Lett.*, **47**(9), ISSN 19448007 (doi: 10.1029/2019GL086926)
- Clancy R, Bitz CM, Edward BW, McGraw MC and Cavallo SM (2022) A Cyclone-Centered Perspective on the Drivers of Asymmetric Patterns in the Atmosphere and Sea Ice during Arctic Cyclones. *J. Clim.*, **35**(1), ISSN 15200442 (doi: 10.1175/JCLI-D-21-0093.1)
- Dowdeswell JA, Hagen JO, Björnsson H, Glazovsky AF, Harrison WD, Holmlund P, Jania J, Koerner RM, Lefauconnier B, Ommanney CSL and Thomas RH (1997) The Mass Balance of Circum-Arctic Glaciers and Recent Climate Change. *Quat. Res.*, **48**(1), 1–14, ISSN 0033-5894 (doi: 10.1006/qres.1997.1900)
- Doyle JG, Lesins G, Thackray CP, Perro C, Nott GJ, Duck TJ, Damoah R and Drummond JR (2011) Water vapor intrusions into the High Arctic during winter. *Geophys. Res. Lett.*, **38**(12), ISSN 00948276 (doi: 10.1029/2011GL047493)
- Duarte P, Sundfjord A, Meyer A, Hudson SR, Spreen G and Smedsrud LH (2020) Warm Atlantic Water Explains Observed Sea Ice Melt Rates North of Svalbard. *J. Geophys. Res. Ocean.*, **125**(8), e2019JC015662, ISSN 2169-9291 (doi: 10.1029/2019JC015662)
- Fearon MG, Doyle JD, Ryglicki DR, Finocchio PM and Sprenger M (2021) The Role of Cyclones in Moisture Transport into the Arctic. *Geophys. Res. Lett.*, **48**(4), ISSN 19448007 (doi: 10.1029/2020GL090353)
- Forbes R, Tompkins AM and Untch A (2011) A new prognostic bulk microphysics scheme for the IFS. *Tech. Mem.*, (649), 22 (doi: 10.21957/bf6vjvxk)
- GLIMS Consortium (2005) GLIMS Glacier Database, Version 1 (doi: http://dx.doi.org/10.7265/N5V98602)
- Goodison BE, Louie PYT and Yang D (1998) WMO solid precipitation measurement intercomparison, WMO/TD No. 872,. Technical report, World Meteorological Organization Publications, Geneva
- Grosvald MG and Kotlyakov VM (1969) Present-Day Glaciers in the U.S.S.R. and Some Data on their Mass Balance. *J. Glaciol.*, 8(52), 9–22, ISSN 0022-1430 (doi: 10.3189/S0022143000020748)

- Haacker J, Wouters B, Fettweis X, Glissenaar IA and Box JE (2024) Atmospheric-river-induced foehn events drain glaciers on Novaya Zemlya. *Nat. Commun.* 2024 15:1, **15**(1), 1–10, ISSN 2041-1723 (doi: 10.1038/S41467-024-51404-8)
- Hagen JO, Kohler J, Melvold K and Winther JG (2003) Glaciers in Svalbard: mass balance, runoff and freshwater flux. *Polar Res.*, **22**(2), 145–159, ISSN 0800-0395 (doi: 10.1111/j.1751-8369.2003.tb00104.x)
- Hall D, Cullather R, DiGirolamo N, Comiso J, Medley B and Nowicki S (2018) A Multilayer Surface Temperature, Surface Albedo, and Water Vapor Product of Greenland from MODIS. Remote. Sens., 10(4), 555, ISSN 2072-4292 (doi: 10.3390/rs10040555)
- Hall DK, Box JE, Casey KA, Hook SJ, Shuman CA and Steffen K (2008a) Comparison of satellite-derived and in-situ observations of ice and snow surface temperatures over Greenland. *Remote. Sens. Environ.*, **112**(10), 3739–3749, ISSN 00344257 (doi: 10.1016/j.rse.2008.05.007)
- Hall DK, Williams RS, Luthcke SB and Digirolamo NE (2008b) Greenland ice sheet surface temperature, melt and mass loss: 2000-06. J. Glaciol., 54(184), 81–93, ISSN 00221430 (doi: 10.3189/002214308784409170)
- Hofsteenge MG, Graversen RG, Rydsaa JH and Rey Z (2022) The impact of atmospheric Rossby waves and cyclones on the Arctic sea ice variability. Clim. Dyn., 59(1-2), ISSN 14320894 (doi: 10.1007/s00382-022-06145-z)
- Hop H, Pearson T, Hegseth EN, Kovacs KM, Wiencke C, Kwasniewski S, Eiane K, Mehlum F, Gulliksen B, Wlodarska-Kowalczuk M, Lydersen C, Weslawski JM, Cochrane S, Gabrielsen GW, Leakey RJG, Lønne OJ, Zajaczkowski M, Falk-Petersen S, Kendall M, Wängberg Sì Bischof K, Voronkov AY, Kovaltchouk NA, Wiktor J, Poltermann M, Prisco G, Papucci C and Gerland S (2002) The marine ecosystem of Kongsfjorden, Svalbard. Polar Res., 21(1), 167–208, ISSN 0800-0395 (doi: 10.1111/j.1751-8369.2002.tb00073.x)
- Hopwood MJ, Carroll D, Dunse T, Hodson A, Holding JM, Iriarte JL, Ribeiro S, Achterberg EP, Cantoni C, Carlson DF, Chierici M, Clarke JS, Cozzi S, Fransson A, Juul-Pedersen T, Winding MHS and Meire L (2020) Review article: How does glacier discharge affect marine biogeochemistry and primary production in the Arctic? *Cryosphere*, **14**(4), 1347–1383, ISSN 1994-0424 (doi: 10.5194/tc-14-1347-2020)
- Hugonnet R, McNabb R, Berthier E, Menounos B, Nuth C, Girod L, Farinotti D, Huss M, Dussaillant I, Brun F and Kääb A (2021) Accelerated global glacier mass loss in the early twenty-first century. *Nature*, **592**(7856), 726–731, ISSN 0028-0836 (doi: 10.1038/s41586-021-03436-z)
- Huss M (2013) Density assumptions for converting geodetic glacier volume change to mass change. Cryosphere, 7, 877–887 (doi: 10.5194/tc-7-877-2013)
- Huss M and Hock R (2018) Global-scale hydrological response to future glacier mass loss. *Nat. Clim. Chang.*, 8(2), 135–140, ISSN 1758-678X (doi: 10.1038/s41558-017-0049-x)

- Innanen SK (2023) Changes in firn properties and meltwater retention on Austfonna ice cap, Svalbard, based on observations and model simulations. Master's thesis, University of Oslo
- Jacob T, Wahr J, Pfeffer WT and Swenson S (2012) Recent contributions of glaciers and ice caps to sea level rise.

 Nature, 482(7386), 514–518, ISSN 00280836 (doi: 10.1038/nature10847)
- Juul-Pedersen T, Arendt K, Mortensen J, Blicher M, Søgaard D and Rysgaard S (2015) Seasonal and interannual phytoplankton production in a sub-Arctic tidewater outlet glacier fjord, SW Greenland. Mar. Ecol. Prog., 524, 27–38, ISSN 0171-8630 (doi: 10.3354/meps11174)
- Kato T and Saito K (1995) Hydrostatic and non-hydrostatic simulations of moist convection: Applicability of the hydrostatic approximation to a high-resolution model. *J. Meteorol. Soc. Japan*, **73**(1), ISSN 00261165 (doi: 10.2151/jmsj1965.73.1 59)
- Kochtitzky W, Copland L, Van Wychen W, Hugonnet R, Hock R, Dowdeswell JA, Benham T, Strozzi T, Glazovsky A, Lavrentiev I, Rounce DR, Millan R, Cook A, Dalton A, Jiskoot H, Cooley J, Jania J and Navarro F (2022) The unquantified mass loss of Northern Hemisphere marine-terminating glaciers from 20002020. *Nat. Commun.*, 13(1), 5835, ISSN 2041-1723 (doi: 10.1038/s41467-022-33231-x)
- Kotlyakov VM, Glazovskii AF and Frolov IE (2010) Glaciation in the Arctic: Causes and effects of global changes (doi: 10.1134/S1019331610020073)
- Lackner G, Domine F, Nadeau DF, Parent AC, Anctil F, Lafaysse M and Dumont M (2022) On the energy budget of a low-Arctic snowpack. *Cryosphere*, **16**, 127–142 (doi: 10.5194/tc-16-127-2022)
- Lang C, Fettweis X and Erpicum M (2015) Stable climate and surface mass balance in Svalbard over 1979–2013 despite the Arctic warming. *Cryosphere*, **9**(1), 83–101, ISSN 1994-0424 (doi: 10.5194/tc-9-83-2015)
- Lenaerts JT, Drew Camron M, Wyburn-Powell CR and Kay JE (2020) Present-day and future Greenland Ice Sheet precipitation frequency from CloudSat observations and the Community Earth System Model. *Cryosphere*, **14**(7), ISSN 19940424 (doi: 10.5194/tc-14-2253-2020)
- Li L, Cannon F, Mazloff MR, Subramanian AC, Wilson AM and Ralph FM (2024) Impact of atmospheric rivers on Arctic sea ice variations. *Cryosphere*, **18**(1), 121–137, ISSN 19940424 (doi: 10.5194/TC-18-121-2024)
- Lind S, Ingvaldsen RB and Furevik T (2018) Arctic warming hotspot in the northern Barents Sea linked to declining sea-ice import. *Nat. Clim. Chang.*, 8(7), 634–639, ISSN 17586798 (doi: 10.1038/s41558-018-0205-y)

- Liu W, Ullrich PA, Guba O, Caldwell PM and Keen ND (2022) An Assessment of Nonhydrostatic and Hydrostatic Dynamical Cores at Seasonal Time Scales in the Energy Exascale Earth System Model (E3SM). *J. Adv. In Model. Earth Syst.*, **14**(2), ISSN 19422466 (doi: 10.1029/2021MS002805)
- Lubinski DJ, Forman SL and Miller GH (1999) Holocene glacier and climate fluctuations on Franz Josef Land, Arctic Russia, 80°N. Technical Report 1 (doi: 10.1016/S0277-3791(97)00105-4)
- Małecki J (2022) Recent contrasting behaviour of mountain glaciers across the European High Arctic revealed by ArcticDEM data. Cryosphere, 16(5), 2067–2082, ISSN 1994-0424 (doi: 10.5194/tc-16-2067-2022)
- Marzeion B, Jarosch AH and Hofer M (2012) Past and future sea-level change from the surface mass balance of glaciers. Cryosphere, 6(6), 1295–1322, ISSN 19940416 (doi: 10.5194/tc-6-1295-2012)
- Maure D, Kittel C, Lambin C, Delhasse A and Fettweis X (2023) Spatially heterogeneous effect of climate warming on the Arctic land ice. *Cryosphere*, **17**, 4645–4659 (doi: 10.5194/tc-17-4645-2023)
- Melkonian AK, Willis MJ, Pritchard ME and Stewart AJ (2016) Recent changes in glacier velocities and thinning at Novaya Zemlya. Remote. Sens. Environ., 174, 244–257, ISSN 00344257 (doi: 10.1016/j.rse.2015.11.001)
- Mémin A, Rogister Y, Hinderer J, Omang OC and Luck B (2011) Secular gravity variation at Svalbard (Norway) from ground observations and GRACE satellite data. *Geophys. J. Int.*, **184**(3), 1119–1130, ISSN 0956540X (doi: 10.1111/j.1365-246X.2010.04922.x)
- Moholdt G, Nuth C, Hagen JO and Kohler J (2010) Recent elevation changes of Svalbard glaciers derived from ICESat laser altimetry. *Remote. Sens. Environ.*, **114**(11), 2756–2767, ISSN 00344257 (doi: 10.1016/j.rse.2010.06.008)
- Moholdt G, Wouters B and Gardner AS (2012) Recent mass changes of glaciers in the Russian High Arctic. *Geophys. Res. Lett.*, **39**(10), n/a–n/a, ISSN 00948276 (doi: 10.1029/2012GL051466)
- Noël B, Jakobs CL, van Pelt WJ, Lhermitte S, Wouters B, Kohler J, Hagen JO, Luks B, Reijmer CH, van de Berg WJ and van den Broeke MR (2020) Low elevation of Svalbard glaciers drives high mass loss variability. *Nat. Commun.*, **11**(1), 1–8, ISSN 20411723 (doi: 10.1038/s41467-020-18356-1)
- Nuth C, Moholdt G, Kohler J, Hagen JO and Kääb A (2010) Svalbard glacier elevation changes and contribution to sea level rise. J. Geophys. Res., 115(F1), F01008, ISSN 0148-0227 (doi: 10.1029/2008JF001223)
- Olonscheck D, Mauritsen T and Notz D (2019) Arctic sea-ice variability is primarily driven by atmospheric temperature fluctuations. *Nat. Geosci.*, **12**(6), ISSN 17520908 (doi: 10.1038/s41561-019-0363-1)
- Østby TI, Schuler TV and Westermann S (2014) Severe cloud contamination of MODIS Land Surface Temperatures over an Arctic ice cap, Svalbard. *Remote. Sens. Environ.*, **142**, 95–102, ISSN 00344257 (doi: 10.1016/j.rse.2013.11.005)

- Østby TI, Vikhamar Schuler T, Ove Hagen J, Hock R, Kohler J and Reijmer CH (2017) Diagnosing the decline in climatic mass balance of glaciers in Svalbard over 1957-2014. *Cryosphere*, **11**(1), 191–215, ISSN 19940424 (doi: 10.5194/tc-11-191-2017)
- Parker CL, Mooney PA, Webster MA and Boisvert LN (2022) The influence of recent and future climate change on spring Arctic cyclones. *Nat. Commun.* 2022 13:1, 13(1), 1–14, ISSN 2041-1723 (doi: 10.1038/S41467-022-34126-7)
- Pfeffer WT, Arendt AA, Bliss A, Bolch T, Cogley JG, Gardner AS, Hagen JO, Hock R, Kaser G, Kienholz C, Miles ES, Moholdt G, Mölg N, Paul F, Radić V, Rastner P, Raup BH, Rich J and Sharp MJ (2014) The Randolph Glacier Inventory: a globally complete inventory of glaciers. *J. Glaciol.*, **60**(221), 537–552, ISSN 0022-1430 (doi: 10.3189/2014JoG13J176)
- Radić V and Hock R (2011) Regionally differentiated contribution of mountain glaciers and ice caps to future sea-level rise. *Nat. Geosci.*, **4**(2), 91–94, ISSN 17520894 (doi: 10.1038/ngeo1052)
- Rastner P, Strozzi T and Paul F (2017) Fusion of Multi-Source Satellite Data and DEMs to Create a New Glacier Inventory for Novaya Zemlya. *Remote. Sens.*, **9**(11), 1122, ISSN 2072-4292 (doi: 10.3390/rs9111122)
- Raup B, Racoviteanu A, Khalsa SJS, Helm C, Armstrong R and Arnaud Y (2007) The GLIMS geospatial glacier database: A new tool for studying glacier change. Glob. Planet. Chang., 56(1-2), 101–110, ISSN 09218181 (doi: 10.1016/j.gloplacha.2006.07.018)
- Royer A, Picard G, Vargel C, Langlois A, Gouttevin I and Dumont M (2021) Improved Simulation of Arctic Circumpolar Land Area Snow Properties and Soil Temperatures. Front. In Earth Sci., 9, 515, ISSN 2296-6463 (doi: 10.3389/feart.2021.685140)
- Schmidt LS (2023) CryoGrid simulations of climatic mass balance and runoff from glaciers in Franz Josef Land and Novaya Zemlya, 1991-2022 [Dataset]. Norwegian Meteorological Institute (doi: 10.21343/k5gq-bh33)
- Schmidt LS, Aðalgeirsdóttir G, Guðmundsson S, Langen PL, Pálsson F, Mottram R, Gascoin S and Björnsson H (2017) The importance of accurate glacier albedo for estimates of surface mass balance on Vatnajökull: evaluating the surface energy budget in a regional climate model with automatic weather station observations. *Cryosphere*, 11(4), 1665–1684, ISSN 1994-0424 (doi: 10.5194/tc-11-1665-2017)
- Schmidt LS, Langen PL, Aðalgeirsdóttir G, Pálsson F, Guðmundsson S and Gunnarsson A (2018) Sensitivity of Glacier Runoff to Winter Snow Thickness Investigated for Vatnajökull Ice Cap, Iceland, Using Numerical Models and Observations. *Atmosphere*, **9**(11), 450, ISSN 20734433 (doi: 10.3390/atmos9110450)
- Schmidt LS, Aðalgeirsdóttir G, Pálsson F, Langen PL, Guðmundsson S, Björnsson H, Aalgeirsdóttir G, Pálsson F, Langen PL, Gumundsson S and Björnsson H (2019) Dynamic simulations of Vatnajökull ice cap from 1980 to 2300. J. Glaciol., 66(255), 97–112, ISSN 00221430 (doi: 10.1017/jog.2019.90)

- Schmidt LS, Schuler TV, Thomas EE and Westermann S (2023) Meltwater runoff and glacier mass balance in the high Arctic: 19912022 simulations for Svalbard. *Cryosphere*, **17**(7), 2941–2963, ISSN 1994-0424 (doi: 10.5194/tc-17-2941-2023)
- Schuler TV, Kohler J, Elagina N, Hagen JOM, Hodson AJ, Jania JA, Kääb AM, Luks B, Małecki J, Moholdt G, Pohjola VA, Sobota I and Van Pelt WJ (2020) Reconciling Svalbard Glacier Mass Balance. Front. In Earth Sci., 8(May), 1–16, ISSN 22966463 (doi: 10.3389/feart.2020.00156)
- Schyberg H, Yang X, Køltzow M, Amstrup B, Bakketun ì Bazile E, Bojarova J, Box J, Dahlgren P, Hagelin S, Homleid M, Horányi A, Høyer J, Johansson ì Killie M, Körnich H, Le Moigne P, Lindskog M, Manninen T, Nielsen Englyst P and Wang Z (2020) Arctic regional reanalysis on single levels from 1991 to present, Copernicus Climate Change Service (C3S) Climate Data Store (CDS) (doi: 10.24381/cds.713858f6)
- Screen JA and Simmonds I (2010) Increasing fall-winter energy loss from the Arctic Ocean and its role in Arctic temperature amplification. *Geophys. Res. Lett.*, **37**(16), n/a-n/a, ISSN 00948276 (doi: 10.1029/2010GL044136)
- Sommer C, Seehaus T, Glazovsky A and Braun MH (2022) Brief communication: Increased glacier mass loss in the Russian High Arctic (2010-2017). Cryosphere, 16(1), 35–42, ISSN 19940424 (doi: 10.5194/tc-16-35-2022)
- Tepes P, Nienow P and Gourmelen N (2021) Accelerating Ice Mass Loss Across Arctic Russia in Response to Atmospheric Warming, Sea Ice Decline, and Atlantification of the Eurasian Arctic Shelf Seas. J. Geophys. Res. Earth Surf., 126(7), e2021JF006068, ISSN 2169-9003 (doi: 10.1029/2021JF006068)
- Van Pelt W, Pohjola V, Pettersson R, Marchenko S, Kohler J, Luks B, Ove Hagen J, Schuler TV, Dunse T, Noël B and Reijmer C (2019) A long-term dataset of climatic mass balance, snow conditions, and runoff in Svalbard (1957-2018). Cryosphere, 13(9), 2259–2280 (doi: 10.5194/tc-13-2259-2019)
- Van Pelt WJ, Oerlemans J, Reijmer CH, Pohjola VA, Pettersson R and Van Angelen JH (2012) Simulating melt, runoff and refreezing on Nordenskiöldbreen, Svalbard, using a coupled snow and energy balance model. *Cryosphere*, **6**(3), 641–659, ISSN 19940416 (doi: 10.5194/tc-6-641-2012)
- Vaughan DG, Comiso JC, Allison I, Carrasco J, Kaser G, Kwok R, Mote P, Murray T, Paul F, Ren J, Rignot E, Solomina O, Steffen K and Zhang T (2013) Observations: Cryosphere. In TF Stocker, D Qin, GK Plattner, M Tignor, SK Allen, J Boschung, A Nauels, Y Xia, V Bex and PM Midgley (eds.), Climate Change 2013: The Physical Science Basis. Contribution of Working Group I to the Fifth Assessment Report of the Intergovernmental Panel on Climate Change, Cambridge University Press, Cambridge, United Kingdom and New York, NY, USA, Cambridge
- Vionnet V, Brun E, Morin S, Boone A, Faroux S, Le Moigne P, Martin E and Willemet JM (2012) The detailed

- snowpack scheme Crocus and its implementation in SURFEX v7.2. Geosci. Model Dev., 5(3), 773–791, ISSN 1991959X (doi: 10.5194/gmd-5-773-2012)
- Wadham JL, De'Ath R, Monteiro FM, Tranter M, Ridgwell A, Raiswell R and Tulaczyk S (2013) The potential role of the Antarctic Ice Sheet in global biogeochemical cycles. Earth Environ. Sci. Trans. R. Soc. Edinburgh, 104(1), 55–67, ISSN 17556929 (doi: 10.1017/S1755691013000108)
- Westermann S, Langer M and Boike J (2011) Spatial and temporal variations of summer surface temperatures of higharctic tundra on Svalbard - Implications for MODIS LST based permafrost monitoring. *Remote. Sens. Environ.*, 115(3), 908–922, ISSN 00344257 (doi: 10.1016/j.rse.2010.11.018)
- Westermann S, Ingeman-Nielsen T, Scheer J, Aalstad K, Aga J, Chaudhary N, Etzelmüller B, Filhol S, Kääb A, Renette C, Schmidt LS, Schuler TV, Zweigel RB, Martin L, Morard S, Ben-Asher M, Angelopoulos M, Boike J, Groenke B, Miesner F, Nitzbon J, Overduin P, Stuenzi SM and Langer M (2023) The CryoGrid community model (version 1.0) a multi-physics toolbox for climate-driven simulations in the terrestrial cryosphere. *Geosci. Model Dev.*, 16(9), 2607–2647, ISSN 1991-9603 (doi: 10.5194/gmd-16-2607-2023)
- Woul MD and Hock R (2005) Static mass-balance sensitivity of Arctic glaciers and ice caps using a degree-day approach. Ann. Glaciol., 42(1), 217–224, ISSN 0260-3055 (doi: 10.3189/172756405781813096)
- Wouters B, Gardner AS and Moholdt G (2019) Global Glacier Mass Loss During the GRACE Satellite Mission (2002-2016). Front. In Earth Sci., 7, 96, ISSN 2296-6463 (doi: 10.3389/feart.2019.00096)
- Yang D, Kane D, Zhang Z, Legates D and Goodison B (2005) Bias corrections of long-term (1973-2004) daily precipitation data over the northern regions. *Geophys. Res. Lett.*, **32**(19), n/a-n/a, ISSN 00948276 (doi: 10.1029/2005GL024057)
- Yang X, Nielsen KP, Amstrup B, Peralta C, Høyer J, Englyst PN, Schyberg H, Homleid M, Køltzow Mì Randriamampianina R, Dahlgren P, Støylen E, Valkonen T, Palmason B, Thorsteinsson S, Bojarova J, Körnich H, Lindskog M, Box J and Mankoff K (2021) C3S Arctic regional reanalysis Full system documentation. Technical report
- Zeeberg J and Forman SL (2001) Changes in glacier extent on north Novaya Zemlya in the twentieth century.

 Holocene, 11(2), 161–175, ISSN 0959-6836 (doi: 10.1191/095968301676173261)

